CrystEngComm

ROYAL SOCIETY OF CHEMISTRY

COMMUNICATION

View Article Online
View Journal | View Issue

Cite this: *CrystEngComm*, 2024, **26**, 5309

Received 26th August 2024,
Accepted 10th September 2024

DOI: 10.1039/d4ce00853g

rsc.li/crystengcomm

The C–I···O halogen bonding in crown ether chemistry†

Weizhou Wang * and Baoming Ji*

The role of the C–I···O halogen bonding in crown ether chemistry has been analyzed and rationalized by using thirteen newly synthesized cocrystals as models. The monotopic C–I···O halogen bonding was found to play a dominant role, whereas the bifurcated halogen bonding and the hydrogen-bond enhanced halogen bonding play minor roles. An unexpected new finding is that some binary mixtures of halogen-bond donor and acceptor can spontaneously absorb trace amounts of water from the solvent during the crystal growth period, forming more complex ternary cocrystals.

In recent years, the halogen bond has been a rising star in the family of noncovalent interactions.[1–7] Like the well-known hydrogen bonding, the halogen bonding is now also becoming a very valuable tool for scientists in various fields ranging from chemistry to material science, biology and even medicine.[2–7] The important role of halogen bonding in supramolecular and macrocyclic chemistry has been explored by many studies.[8–17] The C–I···N halogen bonding is the most common halogen-bonding motif in supramolecular and macrocyclic chemistry because the iodine atom is a strong halogen-bond donor and the nitrogen atom is a strong halogen-bond acceptor. Compared with the C–I···N halogen bonding, the C–I···O halogen bonding is usually much weaker and therefore less applied and studied.[2–17] However, many important macrocyclic compounds, such as crown ethers, cyclodextrins, calixarenes and pillararenes, have only the oxygen heteroatoms, which means that the study of the role of the C–I···O halogen bonding in supramolecular and macrocyclic chemistry is actually very significant. In this work, we systematically studied the role of the C–I···O halogen bonding in crown ether chemistry by selecting the 12-crown-4 (**C4**), 15-crown-5 (**C5**) and 18-crown-6 (**C6**) as the halogen-bond acceptors, and selecting the 1,2-diiodotetrafluorobenzene (**I12**), 1,3-diiodotetrafluorobenzene (**I13**), 1,4-diiodotetrafluorobenzene (**I14**) and 1,3,5-trifluoro-2,4,6-triiodobenzene (**I135**) as the halogen-bond donors (Fig. 1). Evidently, all these halogen-bond donors and acceptors are simple but representative, which ensures that the conclusions of this study are sufficiently general in crown ether chemistry.

Using *n*-heptane as the solvent, we prepared the solutions of binary mixtures of **C4**, **C5** or **C6** with **I12**, **I13**, **I14**, and **I135**, respectively, in 1 : 1 molar ratio by gently stirring in the air at room temperature. After a few days, single crystals of thirteen cocrystals suitable for single-crystal X-ray diffraction analyses were successfully synthesized by slowly evaporating these solutions also in the air and at room temperature. The experimental details, single-crystal structures, crystallographic data, and structure refinement parameters are given in the ESI.†

Fig. 2 shows the halogen bonding motifs which appear in the thirteen crystal structures. Motif **M1** is the monotopic C–I···O halogen bonding; motif **M2** is the bifurcated C–I···(O,O) halogen bonding; motif **M3** is the hydrogen bond enhanced C–I···O halogen bonding;[18] motif **M4** is the monotopic C–I···O(W) halogen bonding in which the O atom of water acts

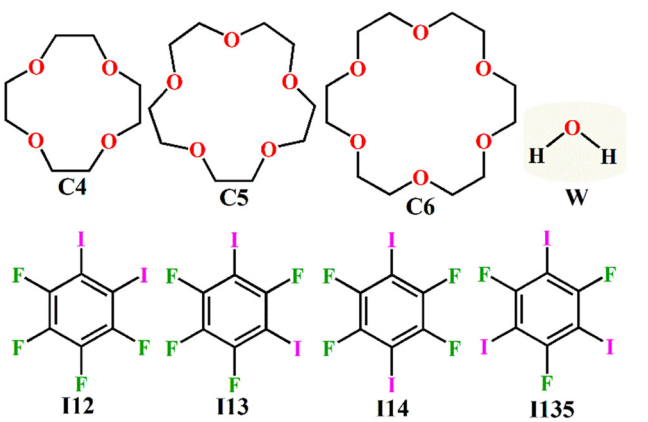

Fig. 1 The halogen-bond donors and acceptors used in this work.

College of Chemistry and Chemical Engineering, Luoyang Normal University, Luoyang 471934, P. R. China. E-mail: wzw@lynu.edu.cn, lyhxxjbm@126.com

† Electronic supplementary information (ESI) available: Details on computational and experimental procedures. CCDC 2281927–2281938 and 2379639. For ESI and crystallographic data in CIF or other electronic format see DOI: https://doi.org/10.1039/d4ce00853g

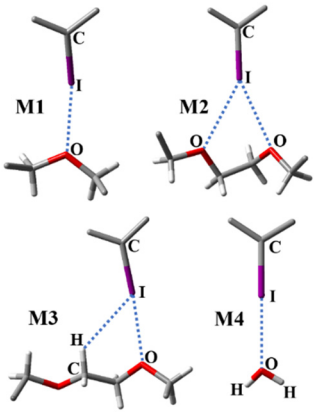

Fig. 2 The halogen bonding motifs found in the thirteen crystal structures.

as the halogen-bond acceptor. In the crystal structures, the most widely used criterion for characterizing a noncovalent bond is that the distance between two nonbonded atoms is smaller than the sum of their van der Waals radii.[19] Here in this study, besides the criterion of interatomic distance, the existence of a noncovalent bond is further identified by employing the theory of "atoms in molecules" (AIM);[20,21] that is to say, a noncovalent bond is considered to be formed only when both criteria are met.

Table 1 lists the stoichiometries and halogen bonding motifs of the thirteen cocrystals. Only three ternary cocrystals, namely, [**C5**][**W**]$_2$[**I13**], [**C6**][**W**]$_4$[**I12**]$_2$ and [**C6**][**W**]$_3$[**I14**] contain the water molecules. In the first round of experiments, the solvent *n*-heptane was used as received and without further dehydration. Finally, we obtained twelve cocrystals excluding [**C6**][**I14**]. After further dehydrating the solvent *n*-heptane, we conducted a second round of experiments. This time, we did not obtain the three water-containing ternary cocrystals but instead obtained a new anhydrous [**C6**][**I14**] cocrystal. Unfortunately, despite multiple attempts, we did not obtain the anhydrous cocrystals [**C5**][**I13**] and [**C6**][**I12**]. Nevertheless, the control experiments with

Table 1 The stoichiometries and halogen bonding motifs in the thirteen cocrystals. The numbers in parentheses are the I···O interatomic distances in Å

	I12	**I13**	**I14**	**I135**
C4	[**C4**][**I12**]$_2$ **M1** (3.013) **M1** (3.130)	[**C4**][**I13**]$_2$ **M1** (2.992) **M1** (3.001)	[**C4**][**I14**]$_2$ **M1** (2.987) **M1** (3.001)	[**C4**][**I135**] **M1** (2.938)
C5	[**C5**][**I12**] **M1** (2.909) **M1** (2.918)	[**C5**][**W**]$_2$[**I13**] **M4** (2.843) **M4** (2.885)	[**C5**][**I14**] **M1** (2.955) **M1** (3.036) **M2** (3.188; 3.308) **M3** (2.919)	[**C5**][**I135**]$_2$ **M1** (2.878) **M1** (3.024) **M3** (3.127)
C6	[**C6**][**W**]$_4$[**I12**]$_2$ **M4** (2.897) **M4** (3.266)	[**C6**][**I13**]$_2$ **M1** (2.940) **M1** (3.141)	[**C6**][**I14**] **M1** (3.062) [**C6**][**W**]$_3$[**I14**] **M1** (2.964) **M4** (2.897)	[**C6**][**I135**]$_2$ **M1** (3.000) **M3** (3.003)

[**C6**][**W**]$_3$[**I14**] and [**C6**][**I14**] clearly indicate that the water molecules in the ternary cocrystals originate from trace amounts of water in the solvent *n*-heptane. None of the cocrystals involving **C4** contain the water molecules. This indicates that the introduction of the water molecules stabilizes the conformation of the much larger crown ether and further facilitates the formation of the cocrystals. Correspondingly, the motif **M4** only exists in the cocrystals [**C5**][**W**]$_2$[**I13**], [**C6**][**W**]$_4$[**I12**]$_2$ and [**C6**][**W**]$_3$[**I14**]. The I···O interatomic distance can be employed to estimate the strength of the C–I···O halogen bonding. The I···O interatomic distances of **M4** are generally shorter than the I···O interatomic distances of **M1**, which shows that motif **M4** is much stronger than motif **M1**. However, as shown in Table 1, motif **M1** is the most commonly seen halogen bonding motif in the thirteen cocrystals. Except for the two cocrystals [**C5**][**W**]$_2$[**I13**] and [**C6**][**W**]$_4$[**I12**]$_2$, all the other cocrystals contain at least one motif **M1**. Like the motif **M4**, motifs **M2** and **M3** are also not commonly found in the thirteen cocrystals. Only one cocrystal contains the motif **M2** and three cocrystals contain the motif **M3** (Table 1). Here, the results clearly show that **M1** will be the dominant halogen bonding motif in crown ether chemistry, although it is not the strongest motif.

The water molecules are not the solvent molecules. Therefore, [**C5**][**W**]$_2$[**I13**], [**C6**][**W**]$_4$[**I12**]$_2$ and [**C6**][**W**]$_3$[**I14**] can be classified as the ternary cocrystals. In 2016, Rissanen and Topić rationally designed and successfully synthesized a series of ternary cocrystals constructed by crown ethers, thioureas and perfluorohalocarbons.[22] Note that the synthesis of higher cocrystals is still a challenging task.[23] In the ternary cocrystals reported by Rissanen and Topić, the C–I(Br)···S halogen bonding between perfluorohalocarbons and thioureas, and the N–H···O hydrogen bonding between thioureas and crown ethers are formed in an orthogonal manner, which makes it possible to develop a strategy for constructing the complex ternary cocrystals. Dang and Yang reported a ternary cocrystal constructed by **C6**, **I14** and acetonitrile in 2020.[24] In this ternary cocrystal, the C–I···N halogen bonding between **I14** and acetonitrile and the C–H···O hydrogen bonding between acetonitrile and **C6** are also orthogonally formed. Here in this work, the role of the water molecule is very similar to that of the thiourea, *N*-methylthiourea or acetonitrile molecule. As shown in Fig. 3, the water molecules are involved in the formations of both the O–H···O hydrogen bonding with **C5**/**C6** and the C–I···O(W) halogen bonding with tetrafluorodiiodobenzene. The formation of the O–H···O hydrogen bonding between water and crown ether sterically hinders the formation of the C–I···O halogen bonding between tetrafluorodiiodobenzene and crown ether, as are the cases in [**C5**][**W**]$_2$[**I13**] and [**C6**][**W**]$_4$[**I12**]$_2$. The exception occurs in [**C6**][**W**]$_3$[**I14**] which still has the C–I···O halogen bonding between **I14** and **C6** (Table 1). This is understandable because there are still two "free" O atoms in **C6** which are not involved in the formation of the O–H···O hydrogen bonding (Fig. 3c).

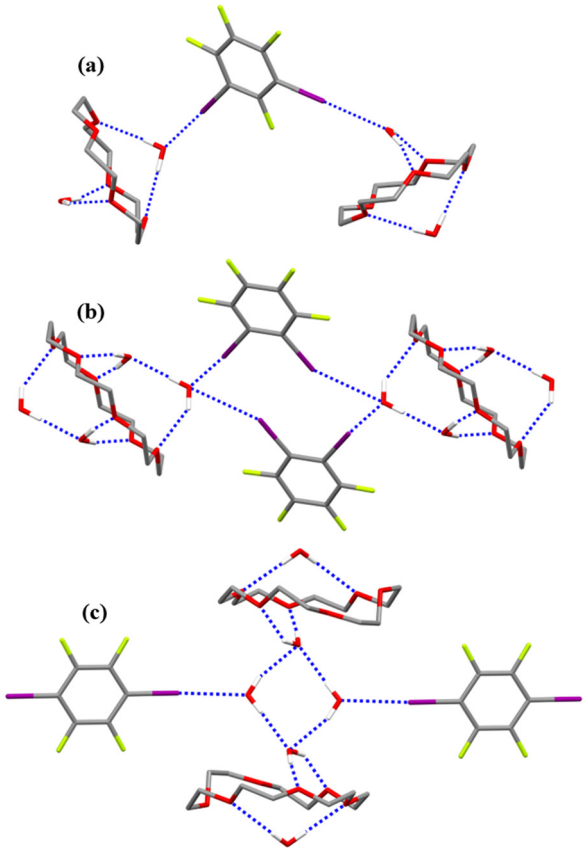

Fig. 3 The C–I···O(W) halogen bonding and O–H···O hydrogen bonding in the cocrystals [**C5**][W]$_2$[**I13**] (a), [**C6**][W]$_4$[**I12**]$_2$ (b) and [**C6**][W]$_3$[**I14**] (c). The hydrogen atoms of **C5** and **C6** are omitted for clarity. The atom colouring scheme: H, white; C, gray; O, red; F, light blue; and I, purple.

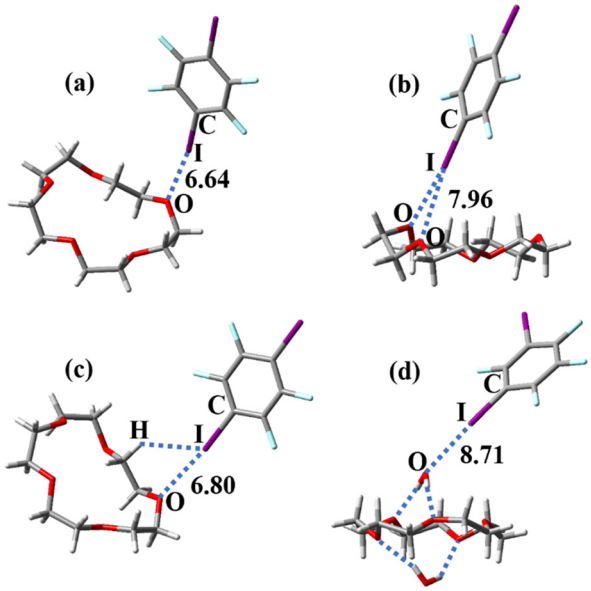

Fig. 4 The binding energies (kcal mol^{-1}) of motifs **M1** (a), **M2** (b), **M3** (c) and **M4** (d) in the cocrystals [**C5**][**I14**] and [**C5**][W]$_2$[**I13**]. The atom colouring scheme: H, white; C, gray; O, red; F, light blue; and I, purple.

The values of the I···O interatomic distances in Table 1 indicate that motif **M4** should be much stronger than motif **M1**. This can be further confirmed by calculating the binding energies of motifs **M1**, **M2**, **M3** and **M4**. The I···O interatomic distance of each motif is slightly different in different cocrystal. The three motifs **M1**, **M2** and **M3** coexist in the cocrystal [**C5**][**I14**], and in the cocrystals involving **C5** only [**C5**][W]$_2$[**I13**] contains the motif **M4**, so the motifs **M1**, **M2** and **M3** in [**C5**][**I14**] and the motif **M4** in [**C5**][W]$_2$[**I13**] were selected to compare their binding strengths (Fig. 4). The bond paths and bond critical points along with the values of electron density Laplacians for the noncovalent bonds in Fig. 4 are given in detail in the ESI† (Section S5). The values of electron density Laplacians for the noncovalent bonds in Fig. 4 are all positive. According to Bader's AIM theory, the positive values of the electron density Laplacians further prove the existence of these noncovalent bonds.[20,21]

The binding energies of the four motifs were calculated at the reliable PBE0-D3(BJ)/def2-TZVPP level of theory.[25–28] The geometries of the dimers in Fig. 4 were taken from the respective crystal structures. All the binding energies have been corrected for the basis set superposition error using the popular counterpoise method.[29] The calculations were carried out with the Gaussian 09 program package.[30] As can be clearly seen in Fig. 4, the binding energies of motifs **M1**, **M2**, **M3** and **M4** are 6.64, 7.96, 6.80 and 8.71 kcal mol^{-1}, respectively. The binding energy of motif **M4** is much larger than that of motif **M1**, which is consistent with the result indicated by the I···O interatomic distances. As expected, motif **M2**, the bifurcated halogen bonding, is stronger than motif **M1** which is the monotopic halogen bonding.[31] The binding energy of motif **M3** is almost the same as that of motif **M1**. This means that the C–I···O halogen bonding in motif **M3** is only slightly enhanced by the weak C–H···I hydrogen bonding.

Politzer, Murray and Clark pointed out in 2010 that the halogen bonding is an electrostatically-driven noncovalent interaction.[32] Therefore, the electrostatic potentials can be used to explain why motif **M4** is much stronger than motif **M1**. Fig. 5 shows the electrostatic potential maps of **C6** and hydrated **C6** calculated at the PBE0-D3(BJ)/def2-TZVPP theory level. The geometries of both **C6** and hydrated **C6** are extracted from the crystal structure of [**C6**][W]$_4$[**I12**]$_2$. In Fig. 5, the O atoms indicated by arrows are the halogen bonding acceptors. In **C6**, the red regions with the most negative electrostatic potentials on the surfaces of the O atoms are located in the center of the molecular ring, and cannot be involved in the formation of the C–I···O halogen bonding due to the steric hindrance. Instead, the yellow regions with less negative electrostatic potentials participate in the formation of the C–I···O halogen bonding. Different from the case in **C6**, the red regions with the most negative electrostatic potentials on the surfaces of the O atoms of the water molecules in hydrated **C6** are directly involved in the formation of the C–I···O(W) halogen bonding. The more negative the electrostatic potential, the stronger the attractive electrostatic force and the stronger the halogen bonding. Apparently, the more negative electrostatic potentials on the

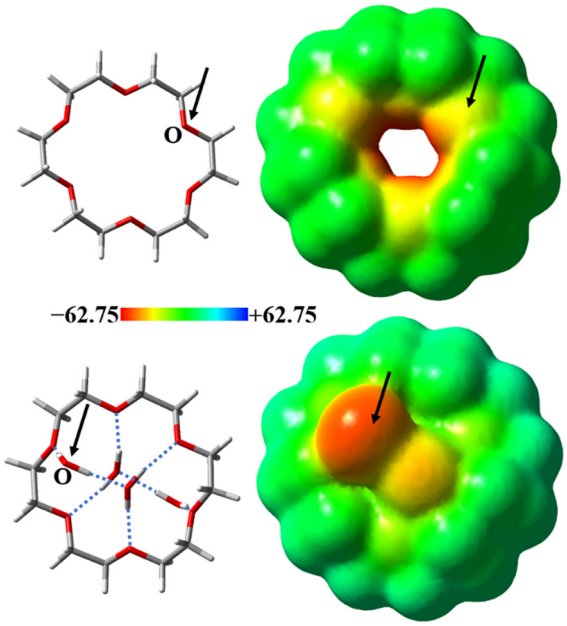

Fig. 5 The electrostatic potential maps of **C6** and hydrated **C6**. The colour scale of electrostatic potential varies from −62.75 (red) to +62.75 (blue) kcal mol^{-1}. The atom colouring scheme: H, white; C, gray; and O, red.

surfaces of the O atoms of the water molecules successfully explain why motif **M4** is much stronger than motif **M1**.

In this study, the role of the C–I···O halogen bonding in crown ether chemistry has been analyzed and rationalized by using a combined experimental and computational approach. The commonly seen monotopic C–I···O halogen bonding was found to play a dominant role in crown ether chemistry, whereas the bifurcated halogen bonding and the hydrogen bond enhanced halogen bonding play minor roles although they are stronger than the monotopic C–I···O halogen bonding. Rather unexpectedly, it was found that some binary mixtures of halogen-bond donor and acceptor can spontaneously absorb trace amounts of water from the solvent during the crystal growth period, which further leads to the formation of more complex ternary cocrystals. There are two factors that drive these binary mixtures to spontaneously absorb the water from the solvent. First, the introduction of the water molecules can stabilize the flexible conformations of **C5** and **C6** *via* strong O–H···O hydrogen bonding. Second, the introduction of the water molecules can facilitate the formations of the cocrystals *via* much stronger C–I···O(W) halogen bonding. This unexpected finding makes it possible to develop a new strategy for constructing the ternary cocrystals involving the macrocyclic compounds.

Data availability

The data supporting this article have been included as part of the ESI.†

Author contributions

WW and BJ conceived and planned the project jointly. WW performed the computations and wrote the first draft. BJ grew crystals and determined the X-ray crystal structures. WW and BJ revised and edited subsequent drafts.

Conflicts of interest

There are no conflicts to declare.

Acknowledgements

This work was supported by the Natural Science Foundation of Henan Province of China (Grant No. 232300421147). The computation resources were provided by China National Supercomputing Center in Shenzhen.

Notes and references

1 G. R. Desiraju, P. S. Ho, L. Kloo, A. C. Legon, R. Marquardt, P. Metrangolo, P. Politzer, G. Resnati and K. Rissanen, *Pure Appl. Chem.*, 2013, **85**, 1711–1713.
2 G. Cavallo, P. Metrangolo, R. Milani, T. Pilati, A. Priimagi, G. Resnati and G. Terraneo, *Chem. Rev.*, 2016, **116**, 2478–2601.
3 P. Metrangolo, L. Canil, A. Abate, G. Terraneo and G. Cavallo, *Angew. Chem.*, 2022, **61**, e202114793.
4 L. Brammer, A. Peuronena and T. M. Roseveare, *Acta Crystallogr., Sect. C: Struct. Chem.*, 2023, **79**, 204–216.
5 W. Wang, Y. Zhang and W. J. Jin, *Coord. Chem. Rev.*, 2020, **404**, 213107.
6 M. R. Scholfield, C. M. V. Zanden, M. Carter and P. S. Ho, *Protein Sci.*, 2013, **22**, 139–152.
7 Z. Xu, Z. Yang, Y. Liu, Y. Lu, K. Chen and W. Zhu, *J. Chem. Inf. Model.*, 2014, **54**, 69–78.
8 L. C. Gilday, S. W. Robinson, T. A. Barendt, M. J. Langton, B. R. Mullaney and P. D. Beer, *Chem. Rev.*, 2015, **115**, 7118–7195.
9 A. V. Jentzsch and S. Matile, *Top. Curr. Chem.*, 2015, **358**, 205–240.
10 M. S. Taylor, *Coord. Chem. Rev.*, 2020, **413**, 213270.
11 A. Priimagi, G. Cavallo, P. Metrangolo and G. Resnati, *Acc. Chem. Res.*, 2013, **46**, 2686–2695.
12 J. Pancholi and P. D. Beer, *Coord. Chem. Rev.*, 2020, **416**, 213281.
13 K. Twum, K. Rissanen and N. K. Beyeh, *Chem. Rec.*, 2021, **21**, 386–395.
14 S. Koppireddi, C.-Z. Liu, H. Wang, D.-W. Zhang and Z.-T. Li, *CrystEngComm*, 2019, **21**, 2626–2630.
15 Y. Xu, C. Liu, H. Wang, D. Zhang and Z. Li, *Chin. J. Org. Chem.*, 2021, **41**, 2848–2860.
16 C. Liu, F. Li, J. Wang, X. Zhao, T. Zhang, X. Huang, M. Wu, Z. Hu, X. Liu and Z. Li, *Acta Chim. Sin.*, 2022, **80**, 1365–1368.

17 B. Hua, L. Shao, M. Li, H. Liang and F. Huang, *Acc. Chem. Res.*, 2022, **55**, 1025–1034.
18 A. M. S. Riel, R. K. Rowe, E. N. Ho, A.-C. C. Carlsson, A. K. Rappé, O. B. Berryman and P. S. Ho, *Acc. Chem. Res.*, 2019, **52**, 2870–2880.
19 A. Bondi, *J. Phys. Chem.*, 1964, **68**, 441–451.
20 R. F. W. Bader, *Atoms in Molecules: A Quantum Theory*, Clarendon, Oxford, UK, 1990.
21 W. Wang, N.-B. Wong, W. Zheng and A. Tian, *J. Phys. Chem. A*, 2004, **108**, 1799–1805.
22 F. Topić and K. Rissanen, *J. Am. Chem. Soc.*, 2016, **138**, 6610–6616.
23 N. A. Mir, R. Dubey and G. R. Desiraju, *Acc. Chem. Res.*, 2019, **52**, 2210–2220.
24 L. Dang and H. Yang, *Z. Kristallogr. - New Cryst. Struct.*, 2020, **235**, 663–664.
25 C. Adamo and V. Barone, *J. Chem. Phys.*, 1999, **110**, 6158–6169.
26 S. Grimme, J. Antony, S. Ehrlich and H. Krieg, *J. Chem. Phys.*, 2010, **132**, 154104.
27 S. Grimme, S. Ehrlich and L. Goerigk, *J. Comput. Chem.*, 2011, **32**, 1456–1465.
28 F. Weigend and R. Ahlrichs, *Phys. Chem. Chem. Phys.*, 2005, **7**, 3297–3305.
29 S. F. Boys and F. Bernardi, *Mol. Phys.*, 1970, **19**, 553–566.
30 M. J. Frisch, G. W. Trucks, H. B. Schlegel, G. Scuseria and M. A. Robb *et al.*, *Gaussian 09, Revision D.01*, Gaussian, Inc., Wallingford, CT, 2009.
31 V. Stilinović, T. Grgurić, T. Piteša, V. Nemec and D. Cinčić, *Cryst. Growth Des.*, 2019, **19**, 1245–1256.
32 P. Politzer, J. S. Murray and T. Clark, *Phys. Chem. Chem. Phys.*, 2010, **12**, 7748–7757.